J. Phys. B: At. Mol. Opt. Phys. **32** (1999) L673–L679. Printed in the UK PII: S0953-4075(99)08264-4

**LETTER TO THE EDITOR**

# Molecular calculation of charge transfer cross sections in $C^{4+}$ + H collisions

L F Errea†, J D Gorfinkiel†, C Harel‡, H Jouin‡, A Macías§, L Méndez†, B Pons‡ and A Riera†

† Departamento de Química C9, Universidad Autónoma de Madrid, Cantoblanco E-28049 Madrid, Spain

‡ Centre Lasers Intenses et Applications (UMR CNRS) Université de Bordeaux I, 351 Cours de la Libération 33405 Talence, France

§ Instituto de Estructura de la Materia CSIC, Serrano 113 bis, 28006 Madrid, Spain

Received 29 September 1999

**Abstract.** We report total and partial charge transfer cross sections for $C^{4+}$ + H collisions in the energy range 0.01–10 keV/amu, calculated using a molecular basis and quantal and semiclassical formalisms. Our total charge transfer cross section does not show the sharp structure found in the experimental measurements of Bliek *et al* (1997 *Phys. Rev.* A **56** 526) at $E \simeq 400$ eV/amu.

Charge transfer in $C^{4+}$ + H collisions is considered as a benchmark system for experimental and theoretical methods for multicharged ion–atom collisions. Experimental work on this system includes the photon emission spectroscopy measurements of Hoekstra *et al* [1] and Dijkkamp *et al* [2], which provided state-selected total cross sections. More recently, Bliek *et al* [3], employed state-of-the-art merged-beam techniques to measure absolute total charge transfer cross sections for impact energies in the range $6 < E < 1000$ eV/amu [3]. The total charge transfer cross section obtained in this last experiment shows a sharp structure at impact energies around 400 eV/amu, which was not found in previous atomic [4] or molecular calculations [5, 6]. The pioneering calculation of [5] used, in a quantal formalism, a model potential approach and a minimal molecular basis with a common reaction coordinate. A semiclassical treatment in [6] is reported, using an expansion on molecular wavefunctions obtained from a pseudopotential calculation. The dynamical treatment of [6] employs the method of Kimura and Lane [8] in which the momentum transfer phases $\exp(\pm i\boldsymbol{v}\cdot\boldsymbol{r})$, with $\boldsymbol{v}$ the relative velocity and $\boldsymbol{r}$ the electron position vector, are removed from the coupling matrix elements (see [9]). The resulting approximate couplings are identical to those obtained when no translation factors are included but with different origins of electronic coordinates for different couplings, and, as a consequence, the coupling matrix is not Hermitian, and the micro-reversibility principle is not fulfilled. In practice, this approximation has been found to artificially flatten the charge transfer cross section in the region of impact energies near its maximum, as can be seen from the illustration given in [10].

The new experimental findings of [3] have motivated the recent work of Tseng and Lin [7] who have recalculated charge transfer cross sections employing a method similar to that of the previous calculation of Fritsch and Lin [4]. Both calculations use a rectilinear trajectory for the relative nuclear motion, and an atomic expansion, which includes plane-wave translation

0953-4075/99/230673+07$30.00  

factors and pseudostates, for the electronic wavefunction. The total charge transfer cross section of [7] agrees with previous atomic calculations of [4] and does not show the sharp structure found in the experiment of [3]

In addition to the controversial sharp structure at $E \simeq 400$ eV/amu, the atomic straight-line trajectory calculations of [7] overestimate the experimental charge transfer cross section [3] by about $5 \times 10^{-16}$ cm$^2$. To explain this difference, Coulomb trajectories were introduced in an approximate way in [7], obtaining better agreement with experiment [3] at low velocities. However, the quantal results of [5] show better agreement with the rectilinear trajectory results of [7] than with the Coulomb trajectory estimate of the same paper. In a recent paper [11], $C^{4+}$ + H charge transfer was used as a test case for the implementation of a time-dependent wavepacket quantum mechanical method, which employs *ab initio* molecular wavefunctions. In [11], electron capture cross sections were calculated for collisions with H and D in the energy range $1 < E < 50$ eV/amu, showing a very small isotopic dependence, which indicates that trajectory effects should also be very small. However, in this work translation factors were not included, and a basis set of only four molecular orbitals (MOs) of $\sigma$ symmetry was employed.

Experimental partial cross sections for charge transfer into $C^{3+}$ ($1s^2\,3l$) [1, 2] show reasonable agreement with the calculations of [4, 5, 7] with the exception of a minimum found by Hoekstra *et al* [1] in the partial cross section into $C^{3+}$ ($1s^2$ 3p) at $E \simeq 150$ eV/amu. In this paper we present a molecular calculation of cross sections for charge transfer in $C^{4+}$ + H collisions, using a large expansion which allows us to ensure convergence. We have also employed both quantal and semiclassical (with rectilinear trajectories) formalisms to discuss the energy range where the latter is applicable.

To evaluate the molecular wavefunctions, we have carried out a configuration interaction (CI) calculation using the program MELD (see, for example, [12]). The numerical differentiation technique of [13], as implemented in [14], was used to evaluate the non-adiabatic couplings. The Gaussian basis set employed in this calculation is similar to the one used in a recent work [15] on $C^{4+}$ + $H_2$ collisions, which accurately describes the molecular states dissociating into $C^{3+}$ ($1s^2\,3l$) + $H^+$. *Ab initio* calculations with a frozen $1s^2$ core yielded energy differences and couplings indistinguishable from those from the full CI. As in previous works [4, 5, 7], we have also calculated the molecular wavefunctions in a single-electron approach where a model potential describes the effect of the $1s^2$ core of the $C^{4+}$ ion. These molecular wavefunctions are then (approximate) eigenfunctions of the one-electron effective Hamiltonian (in atomic units)

$$H_{\rm eff} = -\frac{1}{2}\nabla^2 + V_{\rm mod}(r_{\rm C}) - \frac{1}{r_{\rm H}} \tag{1}$$

where $r_{\rm C}$, $r_{\rm H}$ are the distances from the electron to the C and H nuclei respectively and $V_{\rm mod}(r)$ is a two-parameter model potential

$$V_{\rm mod}(r) = -\frac{4}{r} + \frac{2}{r}(1 + \alpha r)\exp(-\beta r). \tag{2}$$

The parameters $\alpha$, $\beta$ are those employed in [5]. The molecular wavefunctions are expressed as linear combinations of one-electron molecular orbitals (OEDMs) of $BeH^{4+}$, which are eigenfunctions of the Hamiltonian obtained by replacing $V_{\rm mod}$ by $-4/r_{\rm C}$ in (1). In the calculation we have included 35 OEDMs, which are those dissociating into $Be^{3+}$ ($n$ = 2, 3, 4, 5) + $H^+$ and $Be^{4+}$ + H(1s). To improve the basis, a set of 30 Gaussian-type functions (GTOs) centred on the C nucleus was added, yielding a OEDM + GTO basis set similar to that employed recently in [16]. Then, by solving the corresponding secular equation in this basis, we have obtained a set of MOs for the $CH^{4+}$ quasimolecule within the model potential approximation. Model potential energy differences agree with the *ab initio* ones with errors

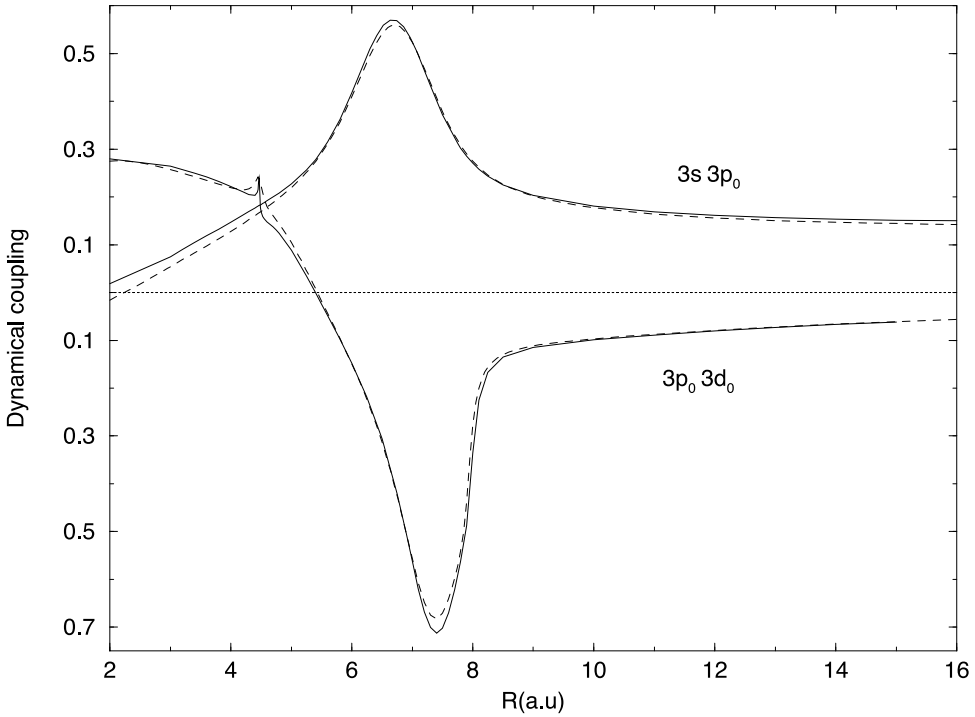


**Figure 1.** Radial couplings $\langle \chi_i | \partial / \partial R | \chi_j \rangle$ between the molecular states dissociating into $C^{3+}$ ($1s^2$ 3s) + $H^+$ and $C^{3+}$ ($1s^2$ $3p_0$) + $H^+$, and $C^{3+}$ ($1s^2$ $3p_0$) + $H^+$ and $C^{3+}$ ($1s^2$ $3d_0$) + $H^+$. Full curve, *ab initio* calculation; dashed curve, model potential calculation. The small peak in the $3p_0$–$3d_0$ is due to an avoided crossing between the energies of the state dissociating into $C^{3+}$ ($1s^2$ $3d_0$) and that of the following adiabatic state.

smaller than $2 \times 10^{-3}$ au. To illustrate the similarity between the corresponding dynamical couplings in figure 1 we have plotted the radial couplings $\langle \chi_i | \partial / \partial R | \chi_j \rangle$, calculated with the origin of electronic coordinates on the H nucleus, between the $\Sigma$ molecular states dissociating into $C^{3+}$ ($1s^2$ $3s\,^2S$) + $H^+$, $C^{3+}$ ($1s^2$ $3p_0\,^2P$) + $H^+$ and $C^{3+}$($1s^2$ $3d_0\,^2D$) + $H^+$, which are the main exit channels. The good comparison between CI and model potential energies and couplings allows us to use the model potential method and thus larger bases.

In the dynamical calculation we have employed both semiclassical and quantal formalisms. In the former case the common translation factor of [17] was included. In the latter case a common reaction coordinate method was used to solve the momentum transfer problem, as explained in [18]; this coordinate is defined in terms of the switching function of [17]. We have carried out calculations using a set of 20 MOs; these are those dissociating into $C^{4+}$ + H(1s) and $C^{3+}$ ($1s^2$ $nl$) + $H^+$ with $n = 2, 3, 4$. To ensure the convergence of our results at high velocities, in the semiclassical calculation we have added 15 MOs dissociating into $C^{3}$+ ($1s^2$ $5l$) + $H^+$, leading to a 35 MO basis set. The convergence is illustrated in table 1 where we compare charge transfer cross sections calculated using the semiclassical formalism and both, 20 and 35 MO, basis sets. Our total cross sections are shown in figure 2, where we have plotted the quantal results for $E < 140$ eV/amu and the semiclassical ones (from the 35 MO calculation) for $E > 140$ eV/amu. In the range 100 eV/amu $< E <$ 10 keV/amu our results agree with those of [4, 5, 7]. The disagreement between our data and those of [6] at $E > 100$ eV/amu is probably due to the approximate method used to calculate the ETF matrix elements in that

**Table 1.** Partial cross sections (in $10^{-16}$ cm$^2$) for charge transfer into $C^{3+}$ ($nl$) levels: (a) 35 MO basis set semiclassical calculation, (b) 20 MO basis set semiclassical calculation, (c) 20 MO basis set quantal calculation.

| $E$(keV/amu) | | 3s | 3p | 3d | $n=3$ | 4s | 4p | 4d | 4f | $n=4$ | Total |
|---|---|---|---|---|---|---|---|---|---|---|---|
| 0.01 | b | 0.02 | 3.48 | 6.78 | 10.28 | 1.14 | 0.99 | 0.20 | 0.10 | 2.43 | 12.71 |
| | c | 0.00 | 3.89 | 5.24 | 9.13 | 0.00 | 0.00 | 0.00 | 0.00 | 0.00 | 9.13 |
| 0.02 | a | 0.09 | 8.31 | 6.11 | 14.51 | 0.69 | 0.96 | 0.20 | 0.21 | 2.06 | 16.58 |
| | b | 0.09 | 8.31 | 6.11 | 14.51 | 0.66 | 0.98 | 0.20 | 0.21 | 2.06 | 16.58 |
| | c | 0.04 | 9.34 | 5.25 | 14.64 | 0.00 | 0.00 | 0.00 | 0.00 | 0.00 | 14.64 |
| 0.04 | b | 0.29 | 16.70 | 3.59 | 20.59 | 0.41 | 1.17 | 0.18 | 0.19 | 1.95 | 22.55 |
| | c | 0.28 | 17.45 | 3.45 | 21.18 | 0.09 | 0.17 | 0.00 | 0.00 | 0.26 | 21.44 |
| 0.06 | a | 0.79 | 22.39 | 2.66 | 25.85 | 0.13 | 0.68 | 0.16 | 0.16 | 1.14 | 26.99 |
| | b | 0.79 | 22.40 | 2.66 | 25.86 | 0.13 | 0.67 | 0.16 | 0.16 | 1.12 | 26.98 |
| | c | 0.66 | 22.73 | 2.42 | 25.82 | 0.12 | 0.43 | 0.01 | 0.00 | 0.57 | 26.38 |
| 0.08 | a | 1.37 | 26.35 | 2.18 | 29.89 | 0.03 | 0.37 | 0.16 | 0.15 | 0.71 | 30.60 |
| | b | 1.37 | 26.37 | 2.17 | 29.91 | 0.03 | 0.36 | 0.16 | 0.14 | 0.70 | 30.61 |
| | c | 1.30 | 26.61 | 1.94 | 30.43 | 0.11 | 0.37 | 0.08 | 0.02 | 0.58 | 30.43 |
| 0.10 | a | 1.67 | 29.40 | 1.99 | 33.06 | 0.01 | 0.21 | 0.23 | 0.11 | 0.56 | 33.62 |
| | b | 1.67 | 29.42 | 1.98 | 33.08 | 0.01 | 0.20 | 0.23 | 0.11 | 0.56 | 33.63 |
| | c | 1.56 | 29.58 | 1.72 | 32.86 | 0.08 | 0.24 | 0.11 | 0.06 | 0.49 | 33.35 |
| 0.14 | a | 3.06 | 31.93 | 2.28 | 37.27 | 0.01 | 0.26 | 0.12 | 0.17 | 0.56 | 37.83 |
| | b | 3.06 | 31.91 | 2.27 | 37.24 | 0.02 | 0.26 | 0.12 | 0.16 | 0.56 | 37.80 |
| | c | 2.97 | 31.83 | 2.00 | 36.80 | 0.02 | 0.19 | 0.08 | 0.12 | 0.42 | 37.21 |
| 0.40 | a | 7.04 | 24.32 | 7.45 | 38.81 | 0.01 | 0.42 | 0.63 | 0.21 | 1.27 | 40.09 |
| | b | 7.01 | 24.35 | 7.49 | 38.85 | 0.03 | 0.43 | 0.62 | 0.19 | 1.27 | 40.13 |
| | c | 7.04 | 24.72 | 6.92 | 38.68 | 0.02 | 0.42 | 0.53 | 0.22 | 1.20 | 39.87 |
| 1.00 | a | 11.89 | 14.53 | 8.91 | 35.33 | 0.23 | 1.02 | 0.54 | 0.24 | 2.04 | 37.44 |
| | b | 11.90 | 14.51 | 8.96 | 35.37 | 0.15 | 1.17 | 0.54 | 0.24 | 2.11 | 37.48 |
| 4.00 | a | 11.36 | 6.99 | 9.43 | 27.77 | 0.11 | 0.43 | 1.56 | 1.18 | 3.28 | 31.45 |
| | b | 11.49 | 7.02 | 9.60 | 28.11 | 0.19 | 0.40 | 1.47 | 1.45 | 3.52 | 31.69 |
| 6.25 | a | 8.40 | 7.13 | 10.24 | 25.77 | 0.36 | 0.60 | 1.61 | 1.68 | 4.25 | 30.87 |
| | b | 8.68 | 7.02 | 10.32 | 26.03 | 0.31 | 0.40 | 1.25 | 2.58 | 4.54 | 30.80 |
| 9.00 | a | 5.08 | 6.64 | 11.54 | 23.26 | 0.43 | 0.59 | 2.15 | 2.97 | 6.14 | 30.80 |
| | b | 5.63 | 6.95 | 11.64 | 24.23 | 0.44 | 0.61 | 1.37 | 3.67 | 6.10 | 30.07 |
| 16.00 | a | 1.93 | 4.77 | 12.65 | 19.35 | 0.42 | 0.88 | 2.17 | 5.44 | 8.90 | 29.91 |
| | b | 2.15 | 5.34 | 12.87 | 20.36 | 0.40 | 1.52 | 1.79 | 4.16 | 7.87 | 28.66 |

work. In addition, our treatment, using larger bases than [5] and a better reaction coordinate (translation factor), allows us to extend the calculation to higher energies and to ensure the accuracy of partial cross sections.

At $E \simeq 10$ keV/amu, ionization starts to be sizeable, as can be seen by extrapolating the experimental results of Shah and Gilbody [19]. Since we have not included pseudostates, $C^{3+}$ ($n = 4, 5$) states are overpopulated in our calculation by the flux that should end up in the ionization continuum. This saturation effect of molecular treatments has been explained in detail in [20], and can be observed in the shape of the total charge transfer cross section in figure 2(*a*), where the increase of this cross section at high energies is of the same order as the above-mentioned ionization cross section. Therefore, our results for the range $10 < E < 25$ keV/amu in figure 2(*a*) correspond to the total cross section for electron loss from the target, and separation of charge transfer and ionization would require the inclusion of pseudostates. On the other hand, the saturation effect does not affect our calculated cross sections into $C^{3+}$ ($n = 3$), as can be observed in the decrease of the cross section at high

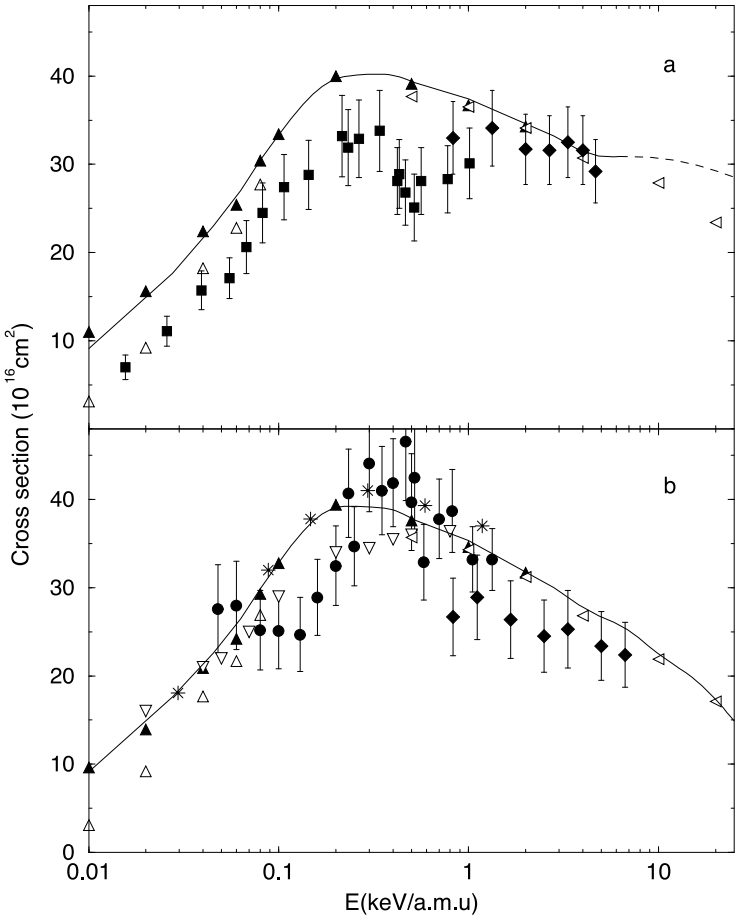


**Figure 2.** (*a*) The total charge transfer cross section compared with other theoretical and experimental results. Present results: full curve, total charge transfer; dashed curve, target electron loss cross section. Other theoretical results: (▲), [7] (straight-line trajectories); (△), [7] (Coulomb trajectories); (◁), [4]. Experimental results: (■), [3]; (♦), [2]. (*b*) Total cross section for charge transfer into $C^{3+}$ ($n = 3$): Full curve: present results. Other theoretical results: (▲), [7] (straight-line trajectories); (△), [7] (Coulomb trajectories); (◁), [4]. (∗), [5]; (▽), [6] (read from the figure in that paper). Experimental results: (○), [1]; (♦), [2].

velocities in figure 2(*b*), and by the agreement with the atomic treatment [4], which includes pseudostates.

Our quantal results and semiclassical results are compared in table 1. From that, we can conclude that quantal effects are small for total charge transfer and partial cross sections into $C^{3+}$ ($1s^2$, $n = 3$), thus agreeing with the conclusion of [11]. However, large differences between quantal and semiclassical cross sections are noticeable for the partial cross sections for electron capture into $C^{3+}$ ($1s^2$, $n = 4$); similar differences between quantal and semiclassical (with rectilinear trajectories) results were found for $Be^{4+}$ + H collisions in [18], where higher cross sections are obtained in the semiclassical case because of transitions taking place at short internuclear distances that are not accessible when deviations from a rectilinear trajectory are allowed. On the other hand, transitions populating the $n = 3$ levels in both systems, $C^{4+}$ and $Be^{4+}$ + H, occur at large impact parameters where these deviations are small. This point

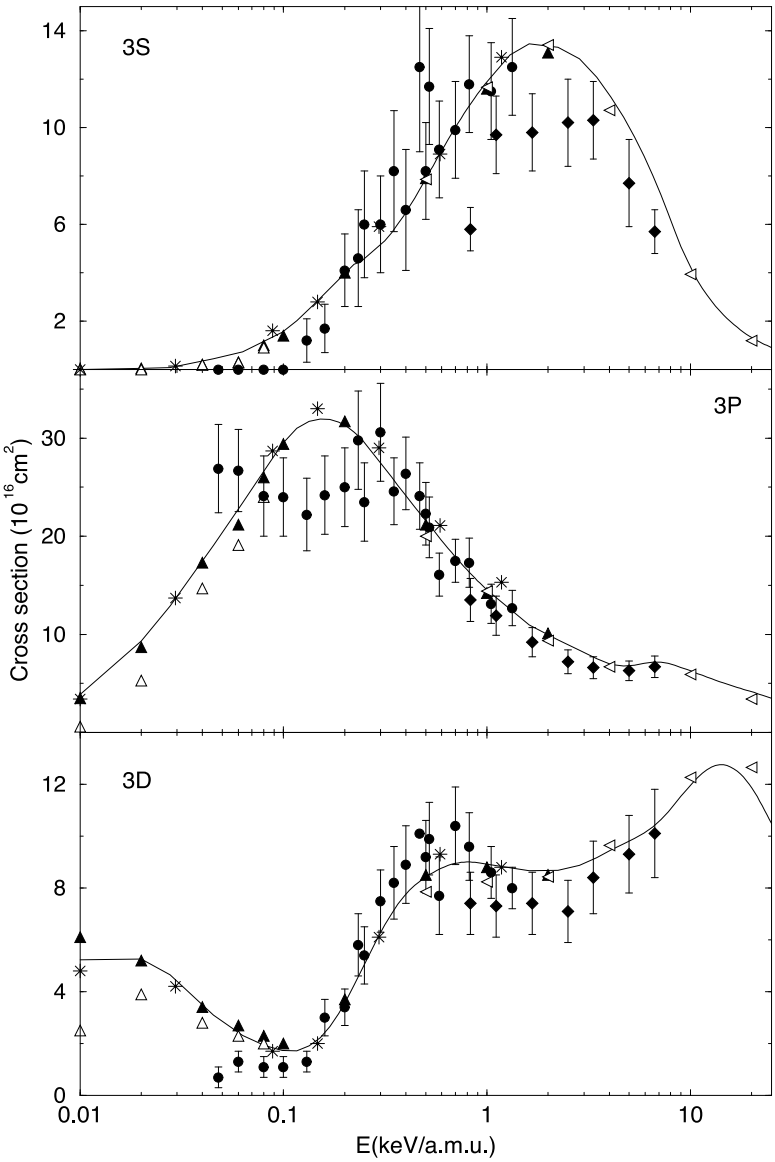


**Figure 3.** Partial charge transfer cross section to 3s, 3p and 3d states of $C^{3+}$. Symbols as in figure 2.

was studied in [18] showing that the use of a single Coulomb trajectory gave rise to incorrect transition probabilities, so that better agreement was found between the quantal results and rectilinear trajectory ones than with the corresponding results from the Coulomb trajectory calculation. Hence, the better agreement of the Coulomb trajectory estimate of Tseng and Lin [7] with experiment is fortuitous. With respect to the comparison with experiments, our total electron capture cross section does not exhibit the sharp structure at $E \simeq 400$ eV/amu found in [3], and at low energies our total cross sections overstimate the experimental ones [3] by about $5 \times 10^{-16}$ cm$^2$. Our results support those of [5] and the rectilinear trajectory atomic results of [7].

Our partial cross sections of figure 3 show general good agreement with those of [1, 2]. However, we do not reproduce the minimum of the experimental cross sections for electron capture into $C^{3+}$ ($1s^2\,3p$) at $E \simeq 150$ eV/amu [1], which is responsible for a dip in the experimental $C^{3+}$ ($1s^2$, $n = 3$) cross section of [1] shown in figure 2(*b*). Since the error bars of the experimental partial cross sections are relatively large, we reckon that this minimum would probably disappear in more precise experiments. At high energies ($E > 200$ eV/amu), our partial cross sections show excellent agreement with those of the atomic plane-wave calculation [4]. At low energies, our results agree with those of [7] (with straight-line trajectories) and [5]. In figure 3 we have not included the low-energy ($100 < E < 200$ eV/amu) results of [4], because these values are inaccurate, as has been pointed out by Tseng and Lin [7].

While the aim of the experimental work of [3] was to establish a benchmark for theoretical predictions, our conclusion is that at this stage the benchmark for $C^{4+}$+H charge transfer is rather provided by state-of-the-art atomic and molecular calculations. In a recent comment [21], we stressed that fully *ab initio* molecular calculations without pseudostates are able to determine charge transfer cross sections of predictive value for impact energies where ionization can be neglected. In this work this condition is fulfilled for the energy range of the experiment performed in [3]. Given the excellent agreement with large-scale atomic calculations (see [7]), we conclude that the limited precision of the experimental measurements is probably responsible for the structures found in charge transfer cross sections at 400 eV/amu in [3] and at 150 eV/amu in [1].

This work has been partially supported by DGICYT project No PB960058.

## References

[1] Hoekstra R, Beijer J P M, Schlatmann A R, Morgenstern R and de Heer F J 1990 *Phys. Rev.* A **41** 4800
[2] Dijkkamp D, Ciric D, Vlieg E, Deboer A and de Heer F J 1985 *J. Phys. B: At. Mol. Phys.* **18** 4763
[3] Bliek F W, Hoekstra R, Bannister M E and Havener C C 1997 *Phys. Rev.* A **56** 426
[4] Fritsch W and Lin C D 1984 *J. Phys. B: At. Mol. Phys.* **17** 3271
[5] Gargaud M, McCarroll R and Valiron P 1987 *J. Phys. B: At. Mol. Phys.* **20** 1555
[6] Saha B C 1995 *Phys. Rev.* A **51** 5021
[7] Tseng H C and Lin C D 1998 *Phys. Rev.* A **58** 1966
[8] Kimura M and Lane N F 1989 *Advances in Atomic, Molecular and Optical Physics* vol 26, ed D R Bates and B Bederson (New York: Academic) p 79
[9] Bates D R and McCarroll R 1958 *Proc. R. Soc.* **245** 175
[10] Errea L F, Harel C, Jouin H, Maidagan J M, Méndez L, Pons B and Riera A 1992 *Phys. Rev.* A **46** 5617
[11] Vaeck N, Desouter-Lecomte M and Liévin J 1999 *J. Phys. B: At. Mol. Opt. Phys.* **32** 409
[12] Davidson E R 1990 *Modern Techniques in Computational Chemistry* ed E Clementi (Leiden: ESCOM)
[13] Cooper I L 1991 *J. Phys. B: At. Mol. Opt. Phys.* **24** 1517
[14] Castillo J F, Errea L F, Macías A, Méndez L and Riera A 1995 *J. Chem. Phys.* **103** 2113
[15] Errea L F, Gorfinkiel J D, Macías A, Méndez L and Riera A 1999 *J. Phys. B: At. Mol. Opt. Phys.* **32** 1705
[16] Errea L F, Harel C, Illescas C, Jouin H, Méndez L, Pons B and Riera A 1998 *J. Phys. B: At. Mol. Opt. Phys.* **31** 3199
[17] Harel C and Jouin H 1988 *J. Phys. B: At. Mol. Opt. Phys.* **21** 859
[18] Errea L F, Harel C, Jouin H, Méndez L, Pons B and Riera A 1998 *J. Phys. B: At. Mol. Opt. Phys.* **31** 3199
[19] Shah M B and Gilbody H B 1981 *J. Phys. B: At. Mol. Phys.* **14** 2831
[20] Harel C, Jouin H, Pons B, Errea L F, Méndez L and Riera A 1997 *Phys. Rev.* A **55** 2831
[21] Errea L F, Méndez L and Riera A 1995 *J. Phys. B: At. Mol. Opt. Phys.* **28** 907